MICROCOPY RESOLUTION TEST CHART
NATIONAL BUREAU-OF STANDARDS-1963-A
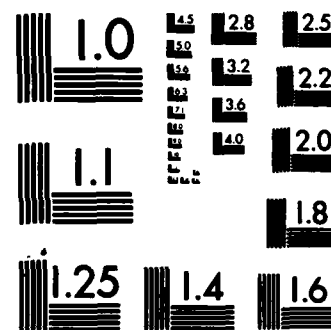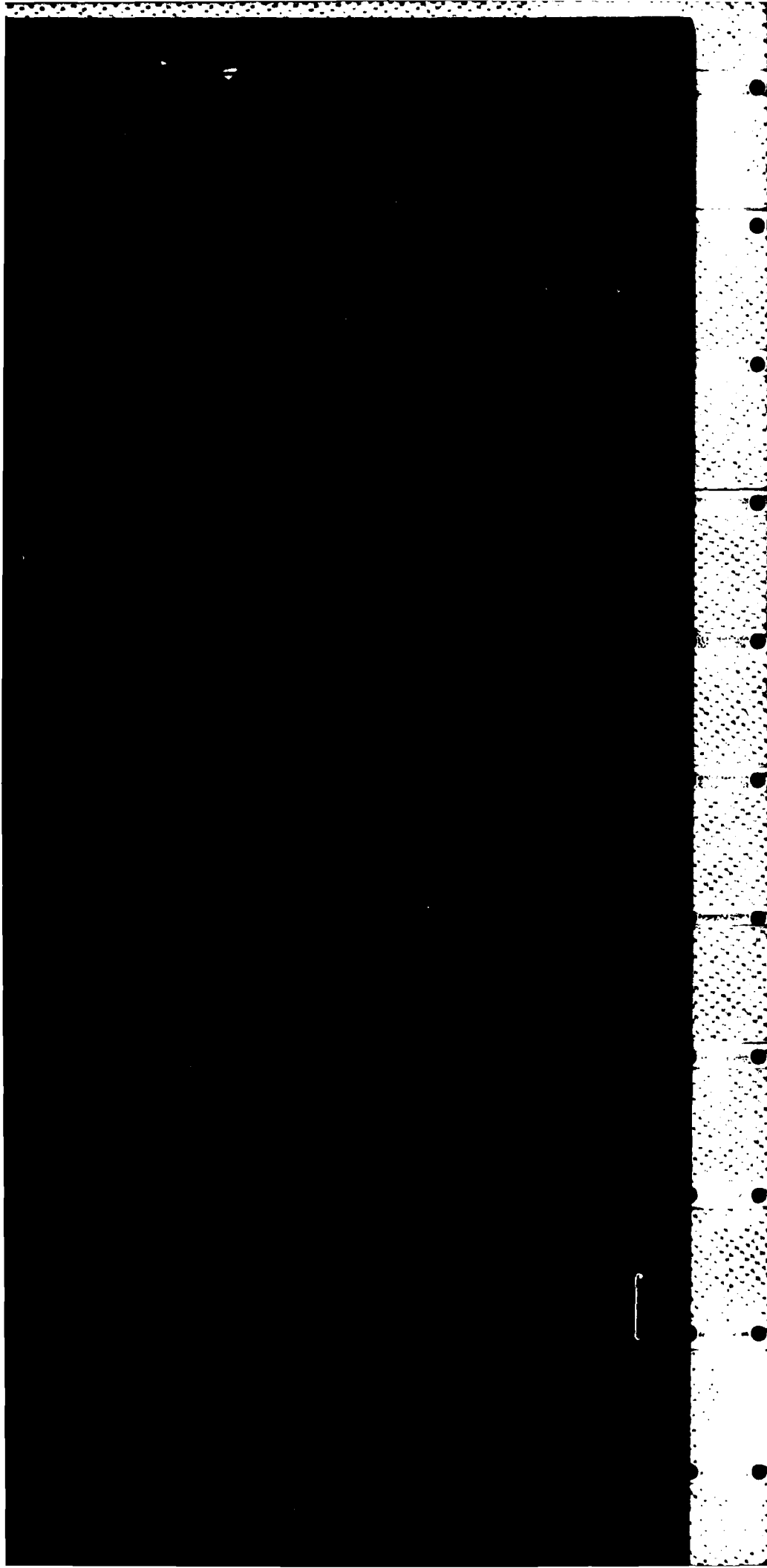
NUMERICAL RESULTS OF ACOUSTIC RADIATION, TRANSMISSION
AND REFLECTION OF STEEL PLATE IN WATER

BY

E.J. CLEMENT

## Summary

Plots of acoustic power versus frequency, and acoustic pressure directivity at selected frequencies, are given for the separate cases of thin, thick and exact plate theories in which the excitation is a vertical time-harmonic point force; they illustrate the range of applicability of the approximate theories. Plots of acoustic power and pressure directivity are given for exact plate theory in which the excitation is a longitudinal force. Plots of pressure transmission and reflection coefficients are given for exact plate theory. Contour and perspective plots of pressure-frequency-angle data, obtained from exact theory, provide vivid illustrations of the acoustic properties of the plate.

## 1. INTRODUCTION

Pestell and James [1] have calculated far-field sound radiation from layered media, excited by time-harmonic forces, by the method of dynamic stiffness coupling in which each element of the system is represented by a 'spectral' dynamic stiffness matrix. Based on this work, Spicer [2] has simplified the mathematical derivation of the stiffness matrices and has included uniform mean subsonic flows in the acoustic fluid elements. Fortran programs arising from the aforementioned studies have been used to predict sound radiation from, and free-wave propagation in, a variety of layered systems. Additionally, a Fortran program has been written to calculate reflection and transmission coefficients due to plane-wave excitation.

The acoustics of fluid-loaded infinite plates has been studied exhaustively in the literature, but only a restricted number of graphical presentations have been published. The mathematics of the 'thin' and 'thick' plate theories can be found in the standard text on fluid-structure interaction [3]. Evseev et al [4] and Sergeev [5] have studied sound radiation using plate theories which include the effects of longitudinal vibrations as formulated by Lyamshev. Freedman [6] gives a limited comparison of the transmission coefficient obtained from exact and approximate plate theories and discusses the effect of including the first symmetric longitudinal wave motion in the thin plate model. Fiorito et al [7] have used a resonance formalism theory which provides physical insight into the peaks and dips that occur in plots of transmission and reflection coefficients versus angle of incidence. Woolley [8] has extended thick plate theory to include symmetric modes of vibration.

It is the purpose of this report to extend the range of published numerical results of sound radiation, reflection and transmission of an infinite steel plate which is immersed in water. Subsequent reports will include numerical results of the acoustics of layered media and will also discuss wavenumber versus frequency plots obtained from the dispersion relation of the layered system. The numerical results contained herein will help to illustrate and aid understanding of the acoustics of a steel plate; they will also provide reference plots for comparisons with plots obtained from simplified theories.

Section 2, below, gives some details of the mathematics needed for both exact and approximate plate theories, the exact theory being based on the multilayer theory of Spicer [2]. The numerical results are discussed in Section 3 and they are followed by some concluding remarks in Section 4.


## 2. MATHEMATICS OF PROBLEM

### (a) Sound Transmission and Reflection, Exact

In Figure 1A a time-harmonic plane-wave is incident on a layered system whose elements are governed by the equations of acoustics, elastodynamics and visco-dynamics. The incident, reflected and transmitted waves must be of the form

$$p_i = P_i \exp(i\alpha x + i\beta y - i\gamma_1 z)$$

$$p_r = P_i R.\exp(i\alpha x + i\beta y + i\gamma_1 z) \qquad (2.1)$$

$$p_t = P_i T.\exp(i\alpha x + i\beta y - i\gamma_2 [z+H])$$

where $P_i$ is the amplitude of the incident wave; R is defined as the complex pressure reflection coefficient; T is defined as the complex pressure transmitted coefficient; $\alpha$, $\beta$, $\gamma_1$ and $\gamma_2$ are wave-numbers which must satisfy the constraints

$$\gamma_1 = +\surd(k_1^2 - \alpha^2 - \beta^2)$$

$$\gamma_2 = +\surd(k_2^2 - \alpha^2 - \beta^2) \qquad (2.2)$$

because the pressures must satisfy the acoustic wave equations in their respective domains; $k_1$ and $k_2$ are acoustic wavenumbers, $\omega/c_1$ and $\omega/c_2$; the time-harmonic factor $\exp(-i\omega t)$ is omitted throughout.

Spicer [2] has presented the mathematics needed to generate the matrix relation connecting interface displacements and forces, viz.

$$[Z(\alpha,\beta)][U(\alpha,\beta)] = [E(\alpha,\beta)] \qquad (2.3)$$
$$M*M \qquad M*1 \qquad M*1$$

where M=3N+3 with N being the number of layers; $[Z(\alpha,\beta)]$ is the system dynamic stiffness matrix;

$$[U(\alpha,\beta)] = [u_{x1}, u_{y1}, u_{z1}, \ldots, u_{xn}, u_{yn}, u_{zn}]^T$$

is a column vector of displacements at the n layer interfaces, where n=N+1;

$$[E(\alpha,\beta)] = [0,0,-2P_i, \ldots ,0,0,0]^T$$

is a column vector of interface stresses, assumed to be positive when acting in the positive z-direction, that takes the above form for plane-wave excitation because the excitation is simply the 'blocked pressure' [3], $-[P_i+P_r]_{z=0}$; the factor $\exp(i\alpha x + i\beta y)$ has been omitted from both sides of the equation.

The normal displacements of the upper and lower surfaces of the system, viz.,

$$U_1(\alpha,\beta) = u_{z1}(\alpha,\beta)\exp(i\alpha x + i\beta y)$$

$$U_2(\alpha,\beta) = u_{zn}(\alpha,\beta)\exp(i\alpha x + i\beta y) \qquad (2.4)$$

are found by matrix inversion of equation (2.3).

The boundary condition

$$[\partial p_i/\partial z + \partial p_r/\partial z]_{z=0} = \rho_1 \omega^2 U_1(\alpha,\beta)$$

that requires continuity of fluid particle and interface displacements at the upper surface gives

$$R = 1 + \rho_1 \omega^2 u_{z1}(\alpha,\beta)/i\gamma_1 P_i \qquad (2.5)$$

and a similar boundary condition applied at $z=-H$ gives

$$T = -\rho_2 \omega^2 u_{zn}(\alpha,\beta)/i\gamma_2 P_i \qquad (2.6)$$

For the particular case shown in Figure 1, the wavenumbers and angle of incidence, $\theta_i$, are related by the simple equations

$$\alpha = k_1 \sin(\theta_i)$$

$$\beta = 0$$

$$\gamma_1 = k_1 \cos(\theta_i)$$

$$\gamma_2 = +\sqrt{[k_2^2 - k_1^2 \sin^2(\theta_i)]}$$

The angle of transmission, $\theta_t$, can be found from Snell's law, viz.

$$k_2 \sin(\theta_t) = k_1 \sin(\theta_i) \qquad (2.7)$$

which gives

$$\theta_t = \tan^{-1}[k_1 \sin\theta_i/(k_2^2 - k_1^2 \sin^2\theta_i)^{1/2}] \qquad (2.8)$$

It may be deduced from equation (2.8) that when $c_1 > c_2$, there is always a real angle of transmission; and when $c_1 < c_2$ there is a critical angle of incidence, $\theta_i = \sin^{-1}(c_1/c_2)$, beyond which there is no transmitted wave. This phenomenon is discussed in numerous texts, for example [9].

The pressure reflection and transmission coefficients in decibels are defined as

$$R_d = 20.0 \times \log_{10}|R|$$
$$\qquad (2.9)$$
$$T_d = 20.0 \times \log_{10}|T|$$

(b) Sound Radiation. Exact

In Figure 2B, time-harmonic point forces and sources excite the layered system, whose far-field pressure in the upper half-space is

$$p(R,\theta,\phi) = -\rho_1 \omega^2 u_{z1}(\alpha,\beta) \exp(ik_1 R)/2\pi R \qquad (2.10)$$

in which the 'stationery phase' [3] wavenumbers are

$$\alpha = k_1 \sin(\theta)\cos(\phi)$$
$$\beta = k_1 \sin(\theta)\sin(\phi) \qquad (2.11)$$

The displacement $u_{z1}(\alpha,\beta)$ is found by matrix inversion of equation (2.3) in which

$$[E(\alpha,\beta)] = [F_{x1}, F_{y1}, F_{z1}, \cdots , F_{xn}, F_{yn}, F_{zn} + S_{zn}]^T$$

A vertical point force, $F_0$, located on the upper interface at $(x=x_0, y=y_0)$, is represented by, for example

$$F_{z1} = F_0 \exp(-i\alpha x_0 - i\beta y_0) \qquad (2.12)$$

and a point source of sound, $p_0 \exp(ik_2 R)/R$, located at distance $z_0$ below the bottom interface gives

$$S_{zn} = 4\pi i p_0 \exp(-i\alpha x_0 - i\beta y_0 + i|z_0|\gamma_2)/\gamma_2 \qquad (2.13)$$

The sound level in dB ref. 1 $\mu N/m^2$ at 1m is defined as

$$dB = 20.0 \times \log_{10} |p(R=1,\theta,\phi)| + 120.0 \qquad (2.14)$$

For the case of point force excitation with peak amplitude $F_0$, the decibels as defined above must be regarded as for force $F_0$ rms.


(c) Sound Radiation of Plate. Approximate

For the special cases of thin and thick (Timoshenko-Mindlin) plate theories the sound pressure is again given by equation (2.10) in which, for point force excitation

$$u_{z1}(\alpha,\beta) = F_0 \exp(-i\alpha x_0 - i\beta y_0)/Z(\alpha,\beta) \qquad (2.15)$$

where

$$Z(\alpha,\beta) = D(\alpha^2+\beta^2)^2 - \omega^2 \rho_s h - i\rho_1 \omega^2/\gamma_1 - i\rho_2 \omega^2/\gamma_2$$

or

$$(2.16)$$

-6-

$$Z(\alpha,\beta) = \{[(D(\alpha^2+\beta^2)-\rho_s h^3\omega^2/12)(\alpha^2+\beta^2-\rho_s\omega^2/KG)-\omega^2\rho_s h]$$

$$/[1+D(\alpha^2+\beta^2)/KGh-\rho_s h^2\omega^2/12KG]\}-i\rho_1\omega^2/\gamma_1-i\rho_2\omega^2/\gamma_2$$

respectively.  D  is the plate flexural rigidity; $\rho_s$  is its density and  h its thickness; G  is  the shear modulus and  $K \simeq \pi^2/12$  is a shear correction factor; $\gamma_1$  and  $\gamma_2$  are given by equation (2.2).  The plate theories are discussed in some detail in the standard text [3] on fluid-structure interaction.

## (d) Power Radiation

The radiated power, in the upper half-space, is defined as

$$P = (1/\rho c) \int_0^{2\pi} \int_0^{\pi/2} |p(R,\theta,\phi)|^2 R^2 \sin(\theta) d\theta d\phi \qquad (2.17)$$

which becomes, on using equation (2.10)

$$P = (\rho\omega^4/4\pi^2 c) \int_0^{2\pi} \int_0^{\pi/2} |u_{z1}(\alpha,\beta)| \sin(\theta) d\theta d\phi \qquad (2.18)$$

For the special case of axisymmetric excitation, it is relatively easy to show that

$$P = (\rho\omega^4/2\pi c) \int_0^{\pi/2} |u_{z1}(\alpha=k_1\sin\theta)|^2 \sin(\theta) d\theta \qquad (2.19)$$

The sound power level in dB ref 1pW is defined as

$$dB = 10.0 \times \log_{10} |P| + 120.0 \qquad (2.20)$$

For the case of point force excitation with peak amplitude  $F_0$,  this definition of power level must be regarded as for force  $F_0$  rms; hence, the customary multiplication factor of one-half has been omitted in equation (2.17).

## 3. NUMERICAL RESULTS

## (a) General

In Figures 2-17, which show transmission, reflection and radiation levels, the following SI constants were used:

Steel plate: $\lambda = 10.437 \times 10^{10}$  $\mu = 7.558 \times 10^{10}$

$E = 19.5 \times 10^{10}$  $\sigma = 0.29$

$\rho_s = 7000.0$  $h = 0.05$


Water: $\rho = 1000.0$  $c = 1500.0$

Plate damping was included in the computations by setting the elastic constants to complex values, for example $E = E(1-i\eta)$, where $\eta$ is called the hysteretic loss factor.


## (b) Acoustic Power

Figures 2 and 3 show acoustic power radiated into the upper half-space by a plate that is excited by a 1kN point force. The lower half-space contains a vacuum. The power levels were obtained via numerical integration of equation (2.19). Small irregularities in the plots are due to the low, but adequate, accuracy of the integrations.

Figures 2A, 2B and 3A form a comparison of power radiated by thin, thick and exact plate theories in which the excitation is applied at the lower surface in the vertical direction. The effects of increasing the damping factor from 0.01 to 0.1 are quantitatively similar on all three plots, viz., a very small effect at frequencies below 5kHz rising to an 8dB reduction at 50kHz. The levels, however, depend on the particular plate theory used; the thin plate theory is inadequate above 5kHz and the thick plate theory is wanting above 40kHz.

A plot of acoustic power radiated by a longitudinal force applied to the lower surface is given in Figure 3B. A comparison of Figures 3A and 3B shows that while the power radiated by a longitudinal force is significantly less at frequencies below 10kHz, it is only about 6dB less than the power radiated by a vertical force at higher frequencies. Because this plot was also obtained via equation (2.19), allowance had to be made for the fact that the pressure varies in the azimuthal direction as $\cos(\phi)$, i.e. this equation was multiplied by one-half.


## (c) Radiated Pressure. Comparison of Theories

Figures 4-9 show the variation with angle $\theta$ of the far-field pressure, at selected frequencies, of the three plate theories. The lower half-space contains a vacuum. The excitation is a 1kN point force which is applied vertically at the lower surface.

At 2kHz, Figure 4, the sound levels of the three theories are virtually identical. They arise from the first antisymmetric branch motion of the plate surface, viz. simple plate flexure. The small notch at 17° in the plot using exact plate theory marks the initial development of significant sound radiation from the first symmetric branch motion of the plate, which is not built into the thin and thick plate equations.

At 5kHz, Figure 5, the 'hump' at $\theta=68°$ marks the development of coinci-

dence lobe radiation: thin plate theory is now no longer suitable. At 10kHz, Figure 6, there is still good agreement between the thick and exact plate theories, except in the region of $\theta=17°$ where the first symmetric branch motion of the exact theory continues its development. At 20kHz, Figure 7, the increasing inadequacy of thick plate theory is evident at $\theta=17°$ and at all angles greater than 45°. At 30kHz, Figure 8, thick plate theory is totally inadequate, except over a small range of angles near to the coincidence lobe at $\theta=36°$.

At 40kHz, Figure 9, the emergence of sound radiation due to the second antisymmetric branch motion of the plate is evident at $\theta=9°$ in both thick and exact plate theories. However, while the thick plate theory is still satisfactory at the coincidence lobe, $\theta=35°$, it does not predict correctly the level of the lobe at $\theta=9°$.

(d) Radiated Pressure. Exact Theory. Longitudinal Force

Figures 10-11 show the variation with $\theta$ of the far-field pressure at selected frequencies for the case of longitudinal point force excitation on the lower surface, which is in contact with a vacuum. The pressure, which varies in the azimuthal direction as $\cos(\phi)$, is plotted at the angle $\phi=0°$.

The sharp peaks at $\theta=17°$ are dominant. When allowance is made for the inadequate resolution of the peaks, the maximum levels are seen to be close to those levels that would have been obtained in the absence of the plate, viz. $20.0 \times \log_{10}(Pf/c) + 120.0$, which range from 182.5dB at 2kHz to 208.5dB at 40kHz. The levels of the broader coincidence lobes, which occur from 10kHz, are only 3-6dB less than the corresponding lobes due to vertical excitation.

(e) Exact Theory. Excitation on Upper Surface

Comparisons have also been made between power and pressure plots obtained from point force excitation on the upper and lower surfaces, respectively, but the plots obtained from the former condition are not included herein. Power levels show only small differences, whereas the pressure levels may differ considerably in the continuum background but not too significantly in regions close to the resonant peaks.

(f) Reflection and Transmission. Exact Theory

Figures 12 and 13 show the reflection and transmission coefficients, respectively, as a function of the angle of incidence, $\theta$. The reflection coefficient is close to 0dB, except at dips which occur at the coincidence angles of the symmetric and antisymmetric branch motions. At 20 and 40kHz, there are well defined peaks in the transmission coefficient at the coincidence angles. The reflection and transmission characteristics of fluid-loaded plates is discussed in some detail in the papers of Freedman [6] and Fiorito [7].

(g) Perspective and Contour Plots. Exact Theory

Figures 14-17 show perspective and contour plots of sound radiation,

reflection and transmission in which the loss factor was chosen as 0.01. They were obtained via the University of Bradford's SIMPLEPLOT graphics package, from a 128×128 array of equispaced decibel data. The perspective plots are for a user-selected angle of view of 60° with the horizontal; their appearance is enhanced by setting a dynamic range of 40dB, that is, values less than the maximum minus 40dB are set to this base level. The perspective plots enable a quick qualitative assessment of the acoustic properties of the steel plate in terms of the two antisymmetric and one symmetric branch motions of the plate. The contour plots present the same information much less vividly, but are more helpful if precise magnitudes are of concern.

## 4. CONCLUDING REMARKS

Numerical results obtained from exact linear theory have been presented for sound radiation, reflection and transmission of a steel plate in water. Some of the plots are new to the literature and should aid physical understanding when studied in conjunction with some of the papers referenced herein. The comparison of sound radiation predictions of thin, thick and exact plate theories have illustrated the range of applicability of the approximate plate theories. The predictions of sound radiation due to longitudinal excitation serve as reference plots for use in the future when predictions obtained from more refined plate theories become available.

E.J. CLEMENT (HSO)

# REFERENCES

1. PESTELL J.L., JAMES J.H., Sound radiation from layered media, Admiralty Marine Technology Establishment, Teddington, AMTE(N)TM79423.

2. SPICER W.J., Free-wave propagation in and sound radiation by layered media with flow, Admiralty Marine Technology Establishment, Teddington, AMTE(N) TM82102.

3. JUNGER M.C., FEIT D., Sound, structures and their interaction, MIT Press, 1972.

4. EVSEEV V.N., et al, Sound radiation by an infinite thin plate driven by a longitudinal force, Sov. Phys. Acoust., 23(5), Sept-Oct. 1977, pages 418-421.

5. SERGEEV Y.D., Influence of shear, rotory inertia, and longitudinal vibrations on the radiation of sound by a point-driven plate, Sov. Phys. Acoust., 25(2), March-April 1979, pages 174-176.

6. FREEDMAN A., Reflectivity and transmitivity of elastic plates. I. Comparison of exact and approximate theories.

7. FIORITO R., et al, Resonance theory of acoustic waves interacting with an elastic plate, J. Acoust. Soc. Am., 66(6), 1979, pages 1857-1866.

8. WOOLLEY B.A., Acoustic radiation from fluid-loaded elastic plates. II. Symmetric modes, J. Acoust. Soc. Am., 72(3), 1982, pages 859-869.

9. DOWLING A.P., FFOWCS-WILLIAMS J.E., Sound and sources of sound, Ellis Horwood, 1983.
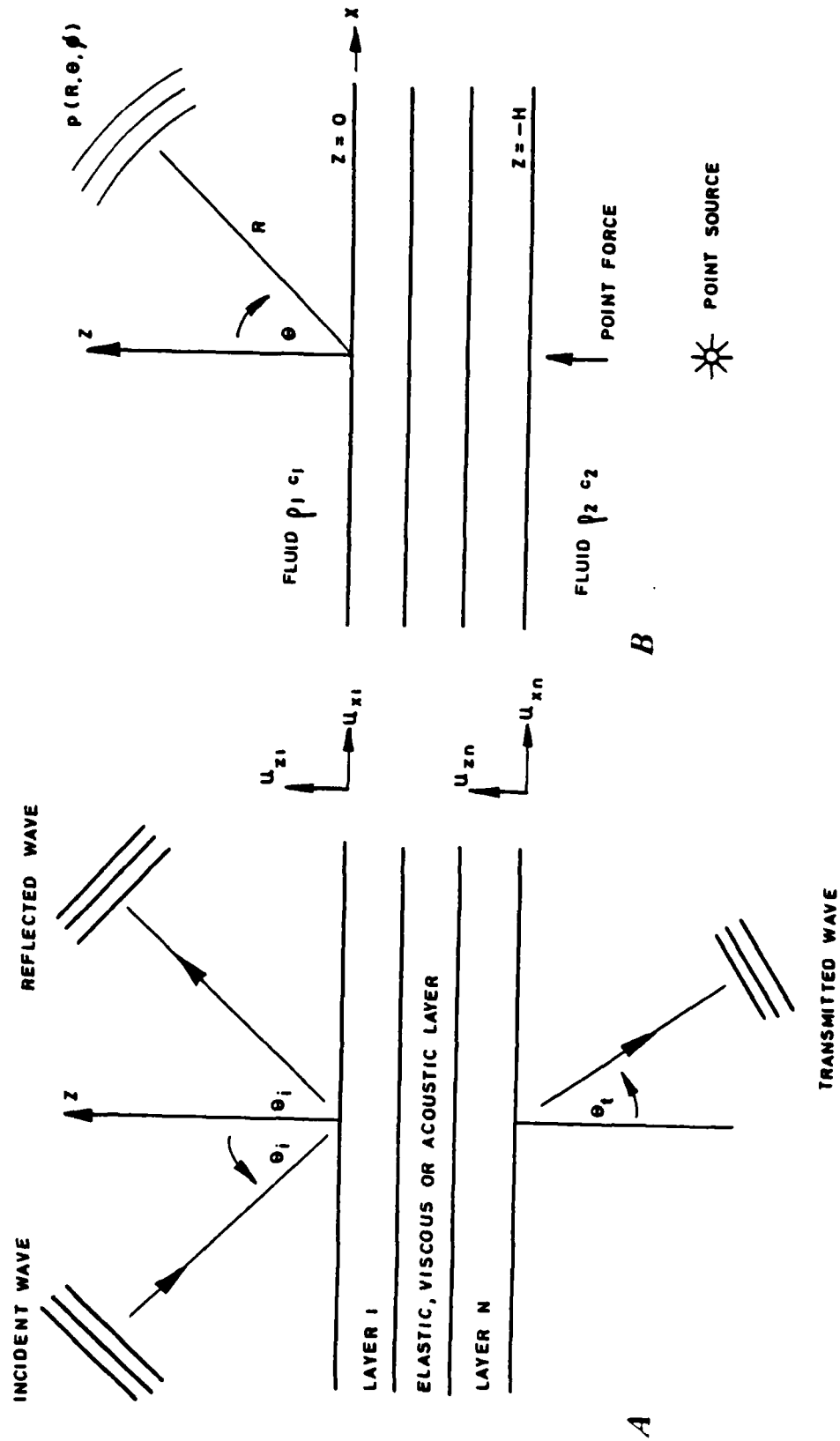
FIG. 1  GEOMETRY FOR TRANSMISSION, REFLECTION AND RADIATION

-13-
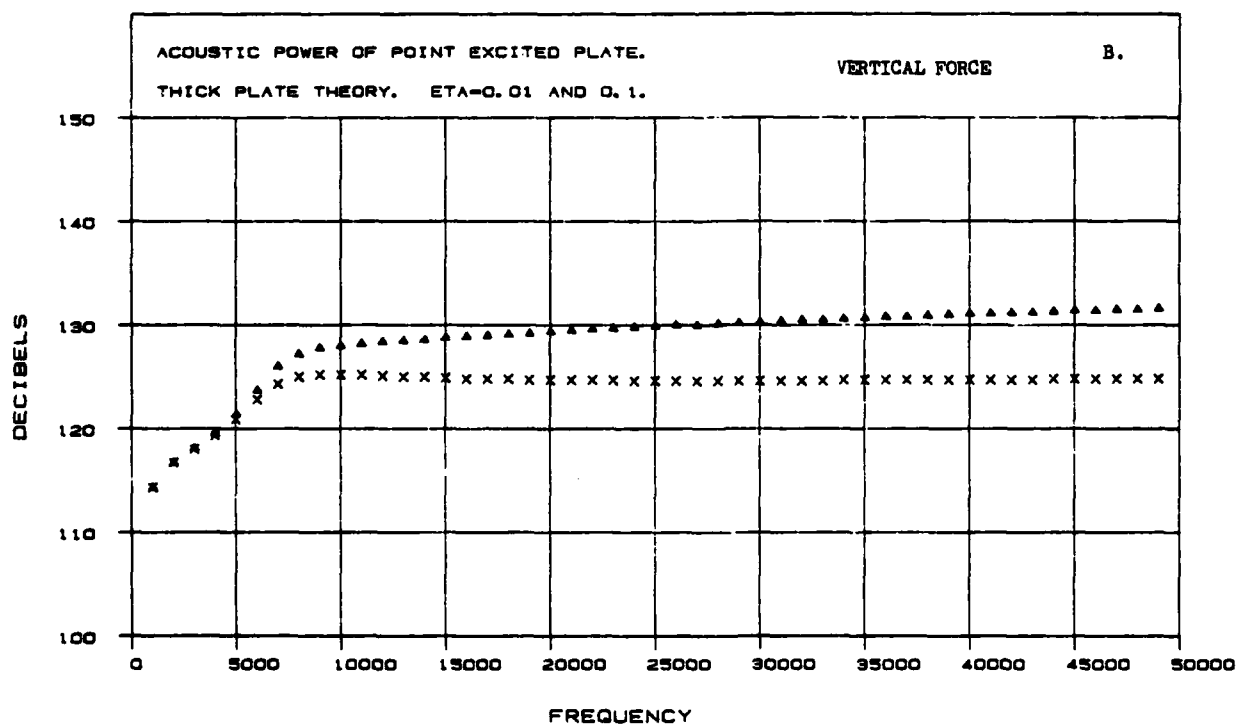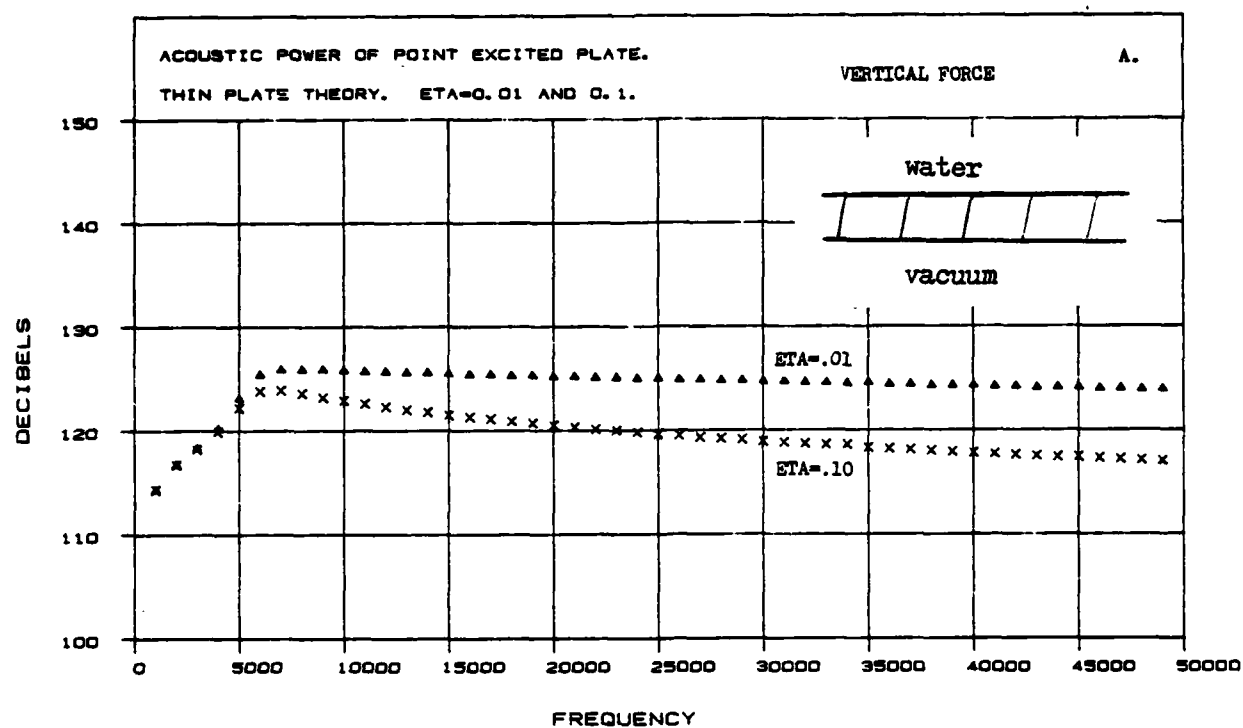
FIG.2 POWER RADIATED BY APPROXIMATE PLATE THEORIES

-14-
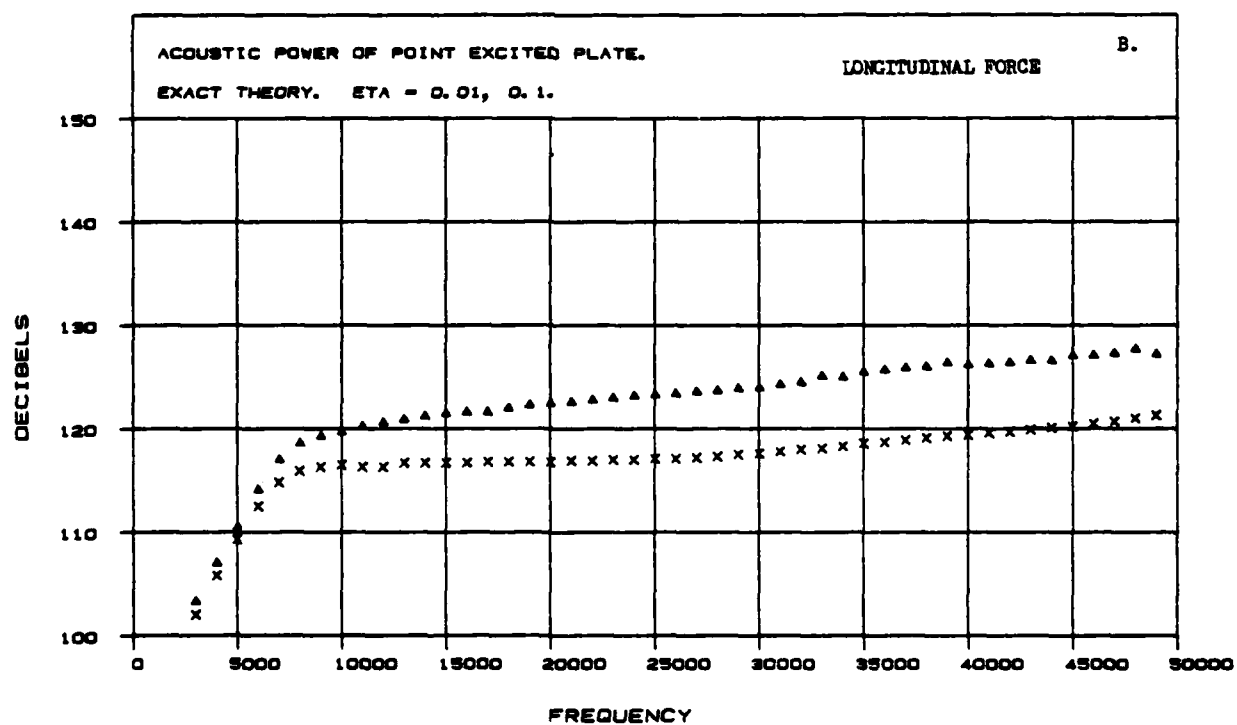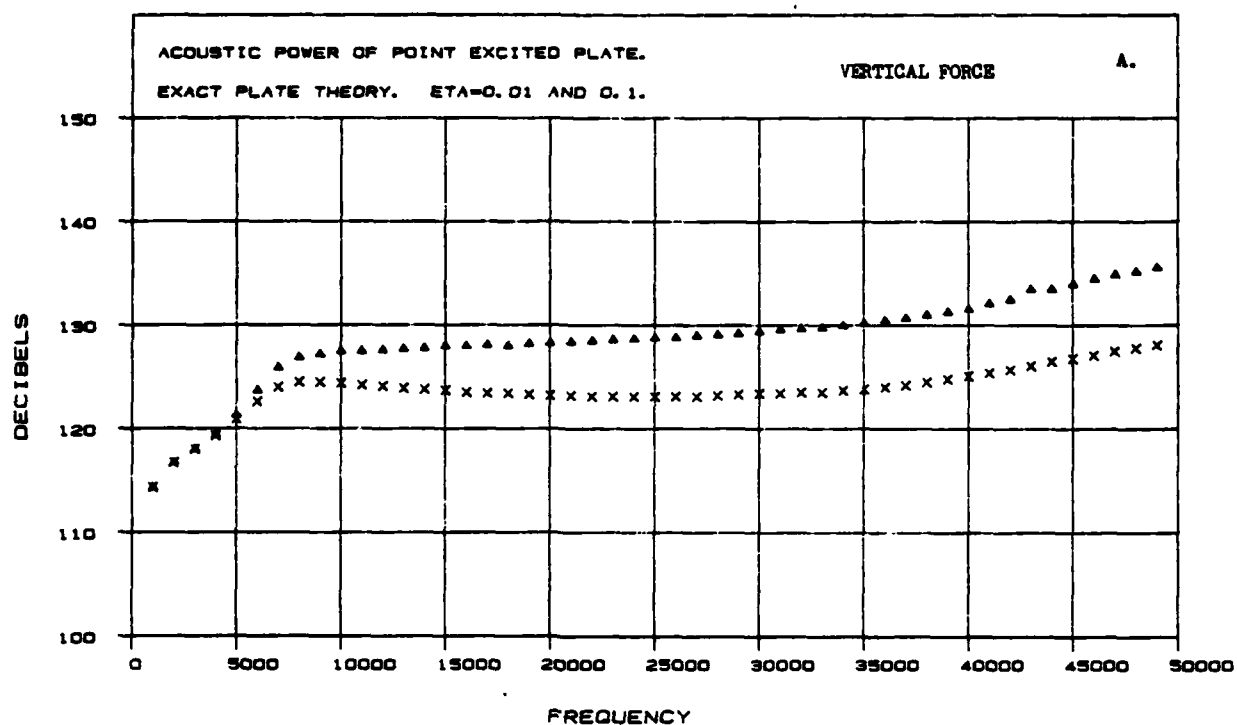
FIG.3  POWER RADIATED BY EXACT PLATE THEORY
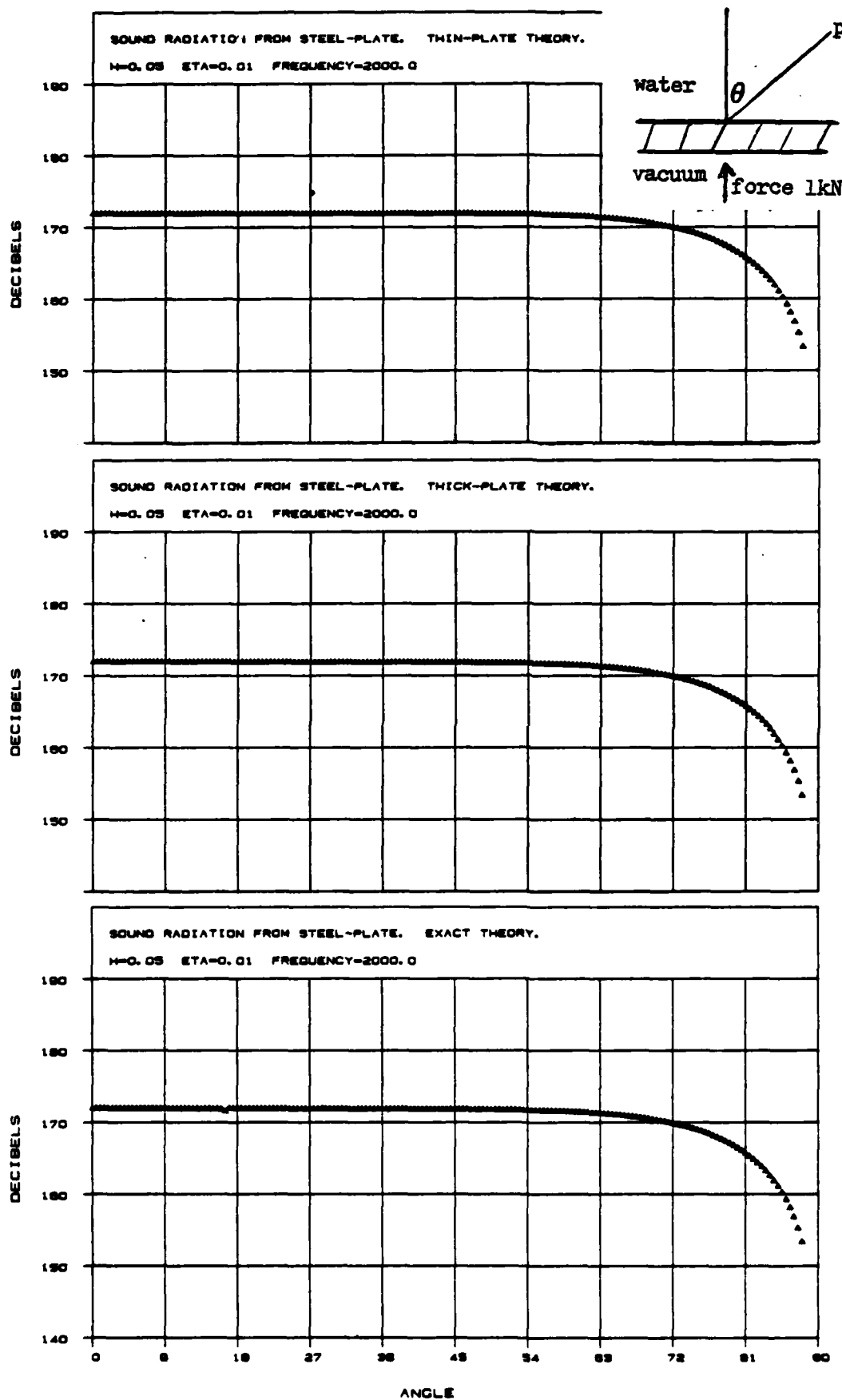
FIG.4  COMPARISON OF SOUND RADIATION AT 2kHz
VERTICAL POINT FORCE ON LOWER SURFACE

-16-

SOUND RADIATION FROM STEEL-PLATE.   THIN-PLATE THEORY.

H=0.05   ETA=0.01   FREQUENCY=5000.0

SOUND RADIATION FROM STEEL-PLATE.   THICK-PLATE THEORY.

H=0.05   ETA=0.01   FREQUENCY=5000.0

SOUND RADIATION FROM STEEL-PLATE.   EXACT THEORY.

H=0.05   ETA=0.01   FREQUENCY=5000.0

ANGLE
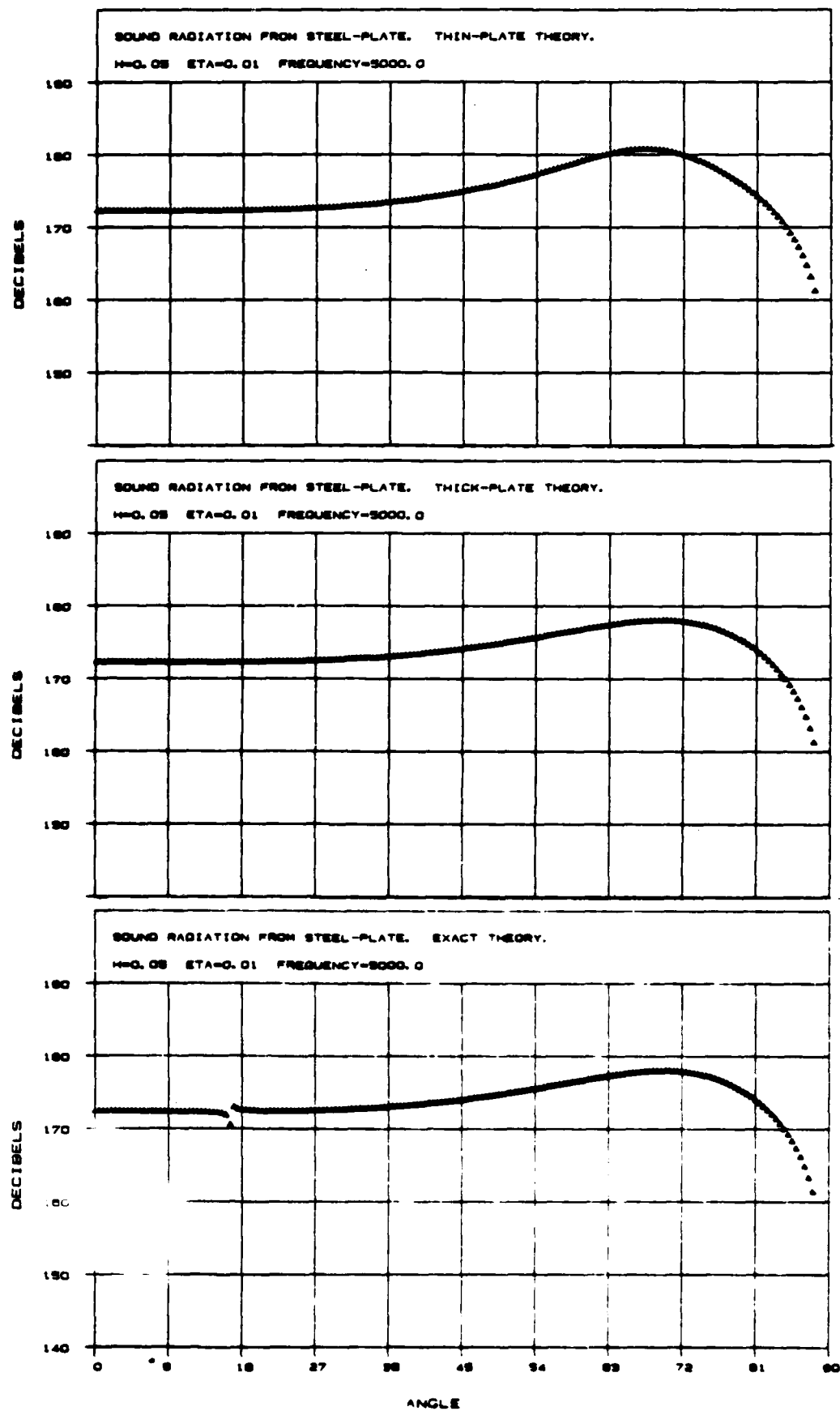
FIG.5   COMPARISON OF SOUND RADIATION AT 5kHz
VERTICAL POINT FORCE ON LOWER SURFACE
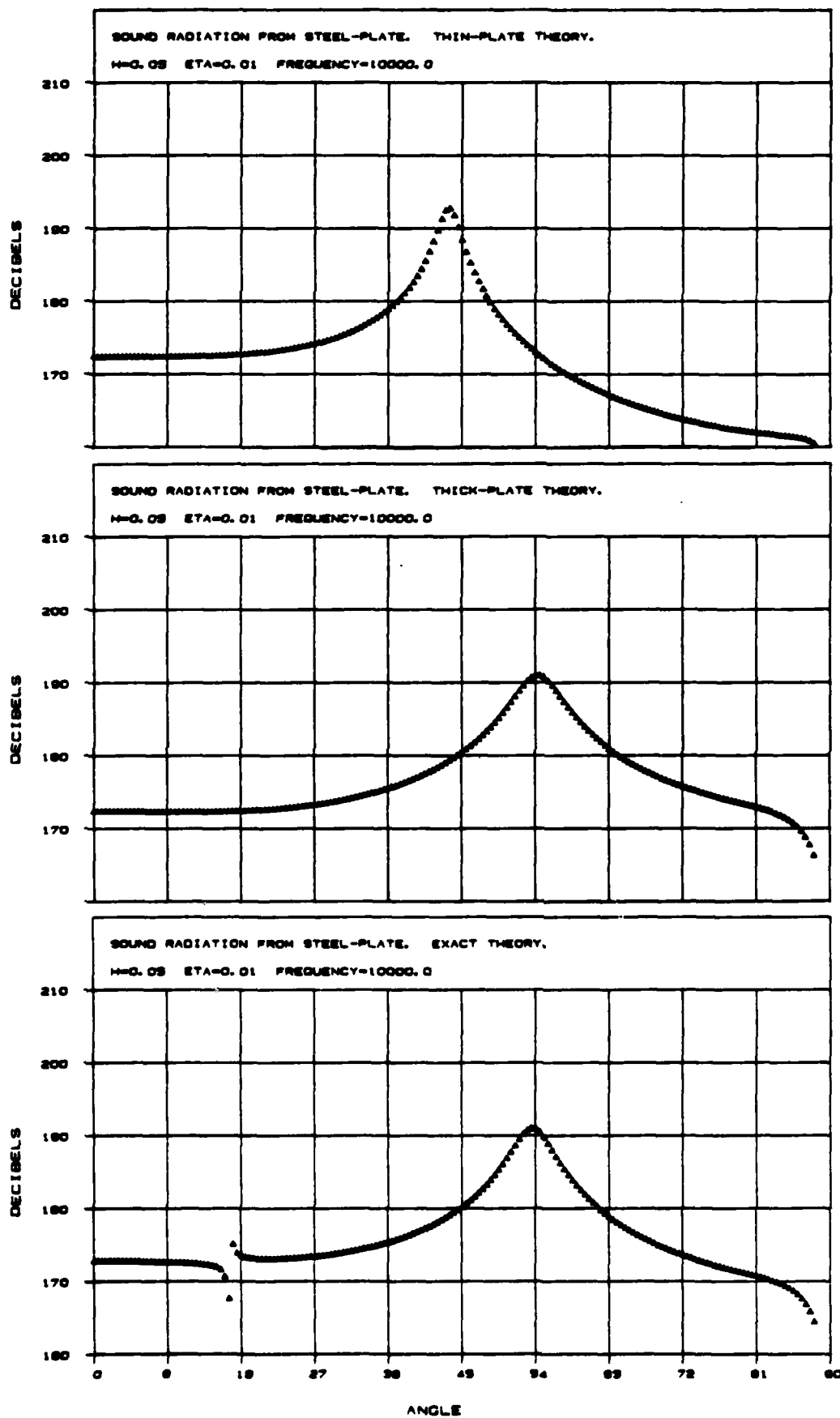
FIG.6  COMPARISON OF SOUND RADIATION AT 10kHz
VERTICAL POINT FORCE ON LOWER SURFACE

-18-
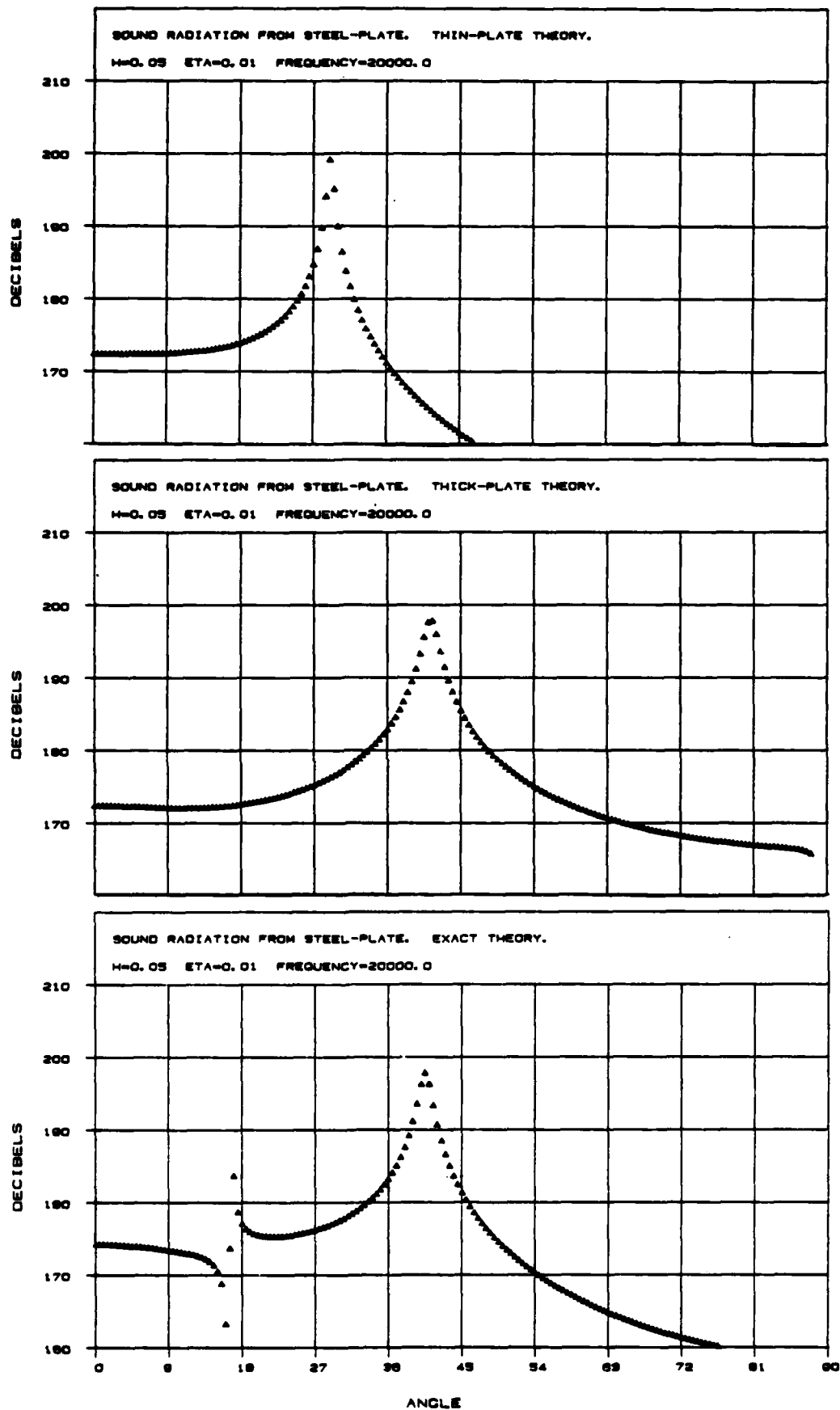
FIG.7 COMPARISON OF SOUND RADIATION AT 20kHz
VERTICAL POINT FORCE ON LOWER SURFACE
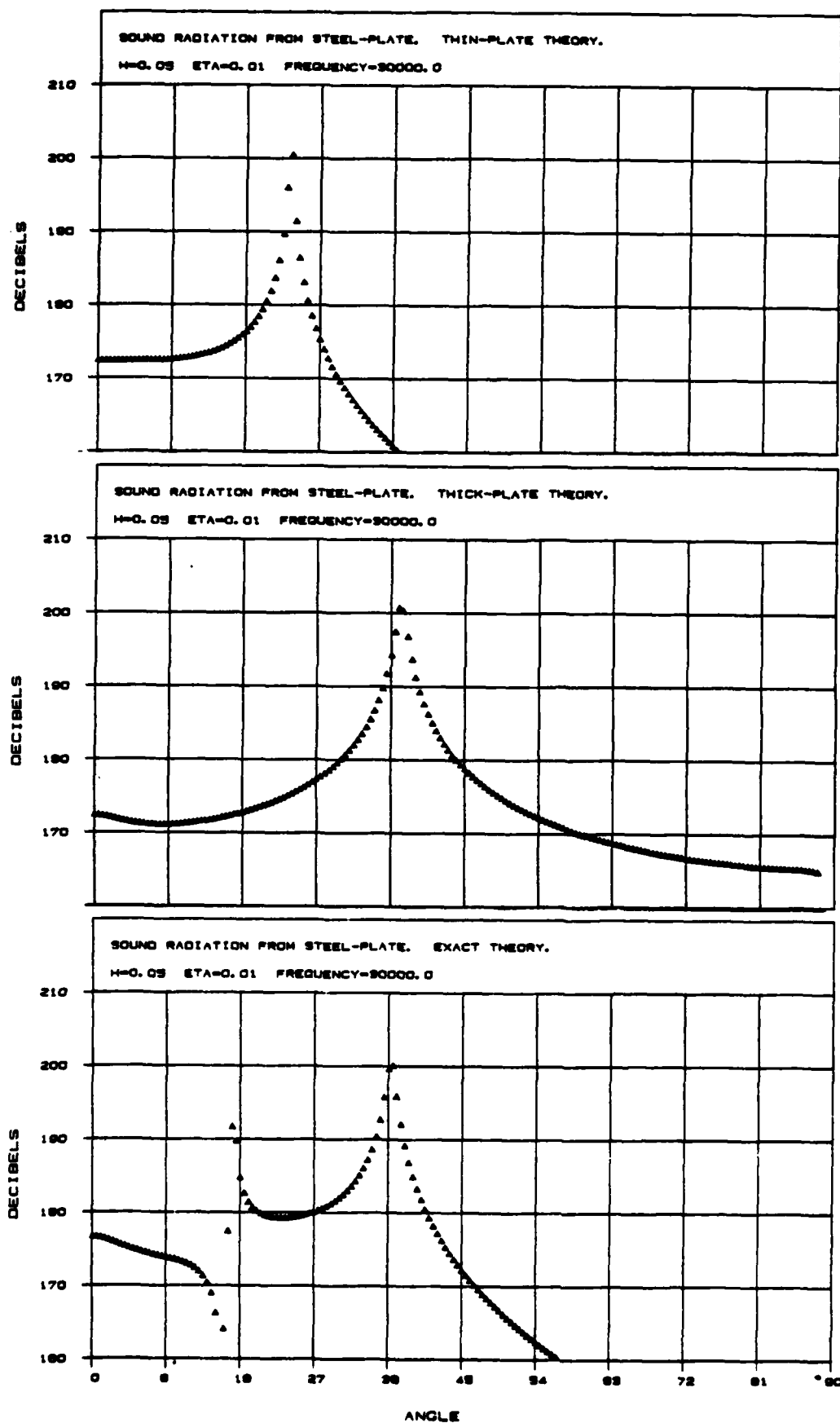
FIG.8  COMPARISON OF SOUND RADIATION AT 30kHz
VERTICAL POINT FORCE ON LOWER SURFACE
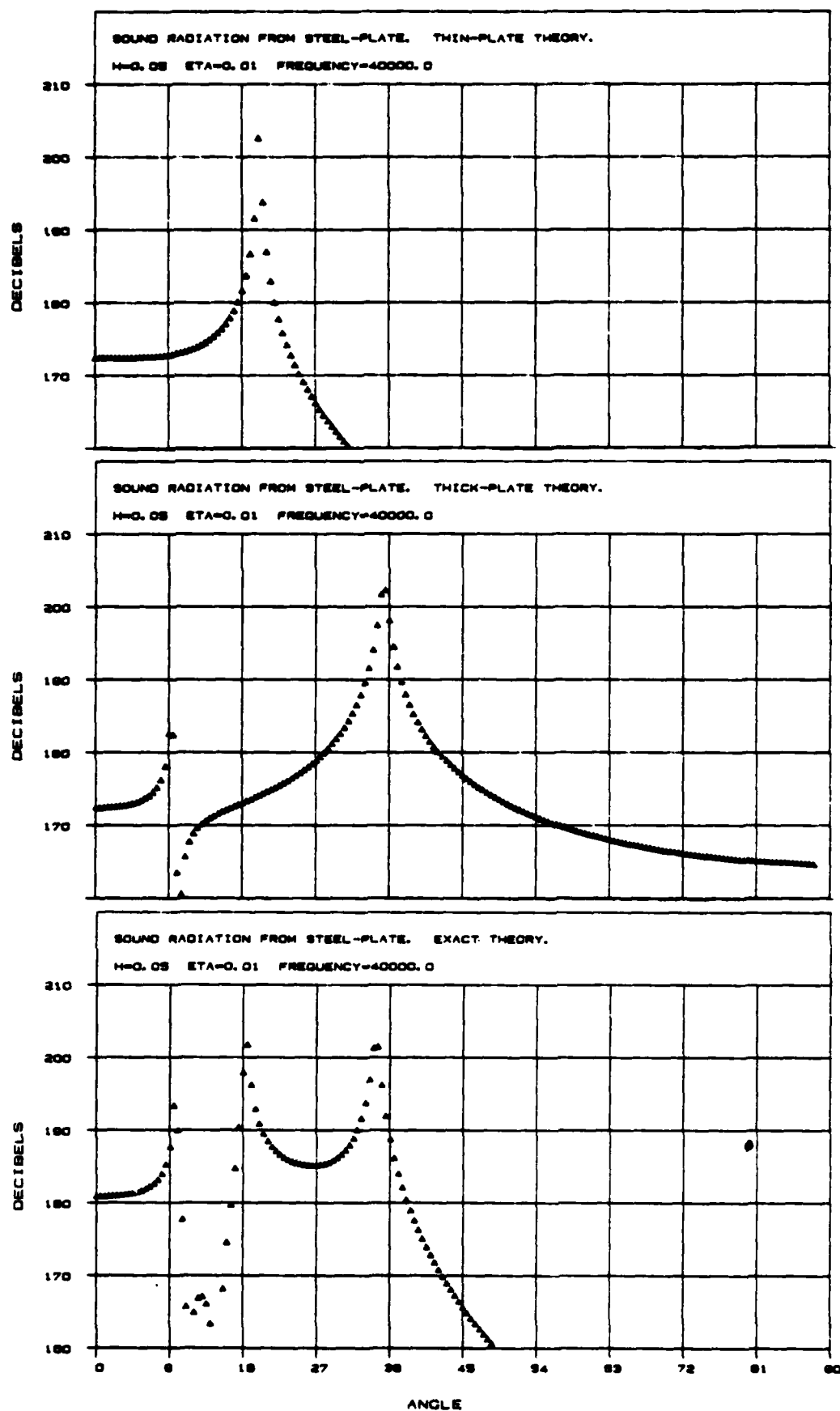
FIG.9  COMPARISON OF SOUND RADIATION AT 40kHz
VERTICAL POINT FORCE ON LOWER SURFACE
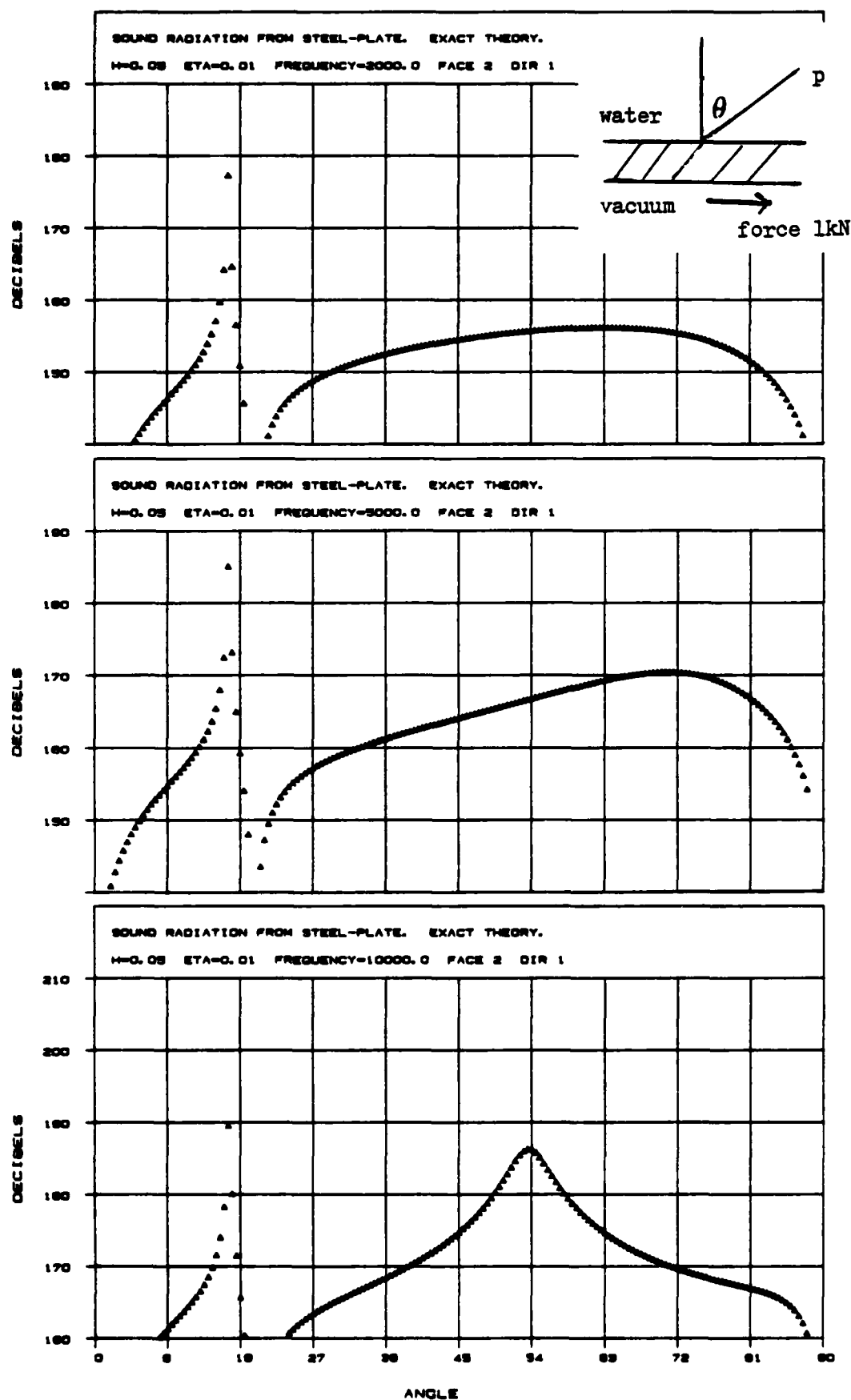
FIG.10 SOUND RADIATION OF EXACT THEORY WITH
LONGITUDINAL FORCE ON LOWER SURFACE

-22-
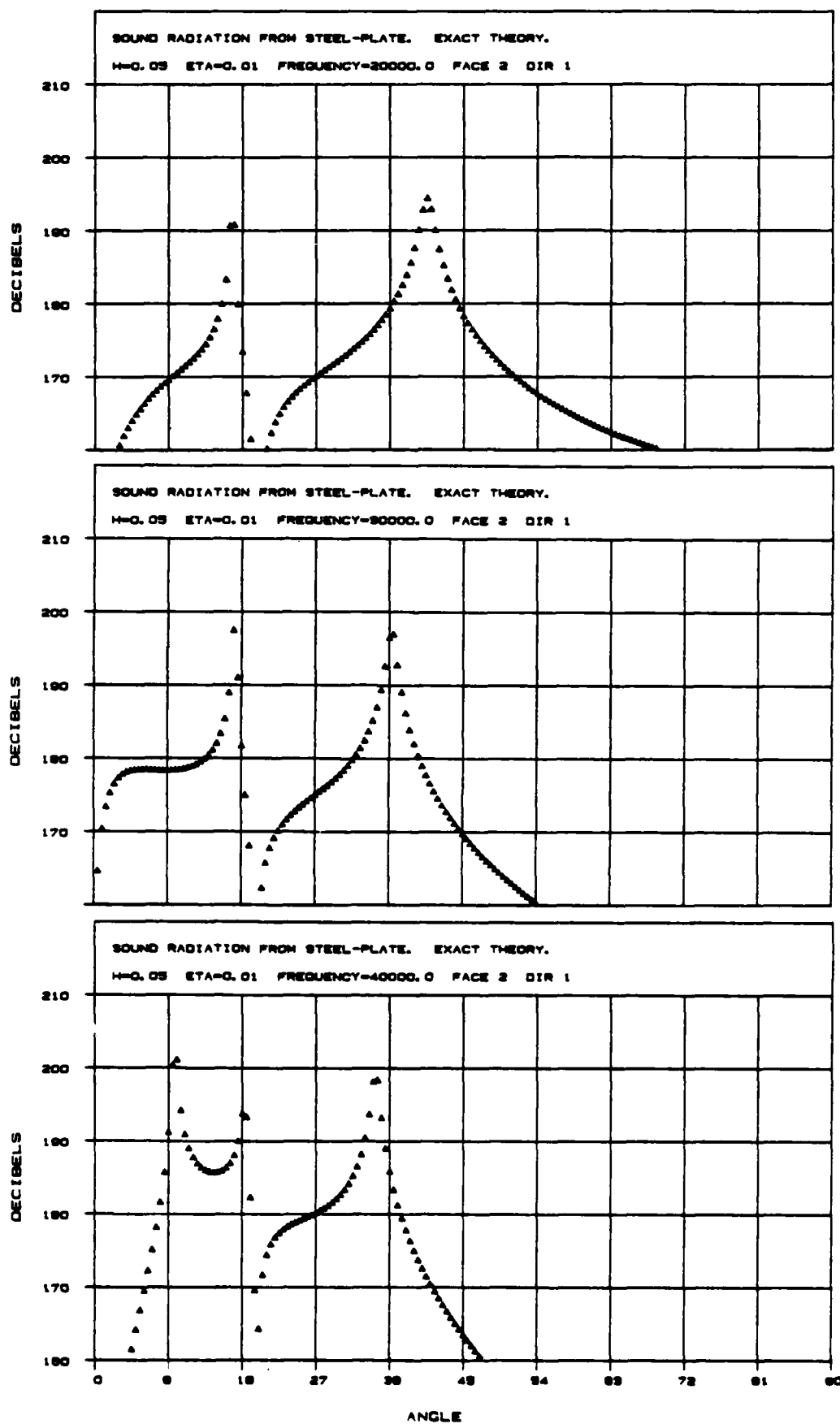
FIG.11  SOUND RADIATION OF EXACT THEORY WITH
LONGITUDINAL FORCE ON LOWER SURFACE
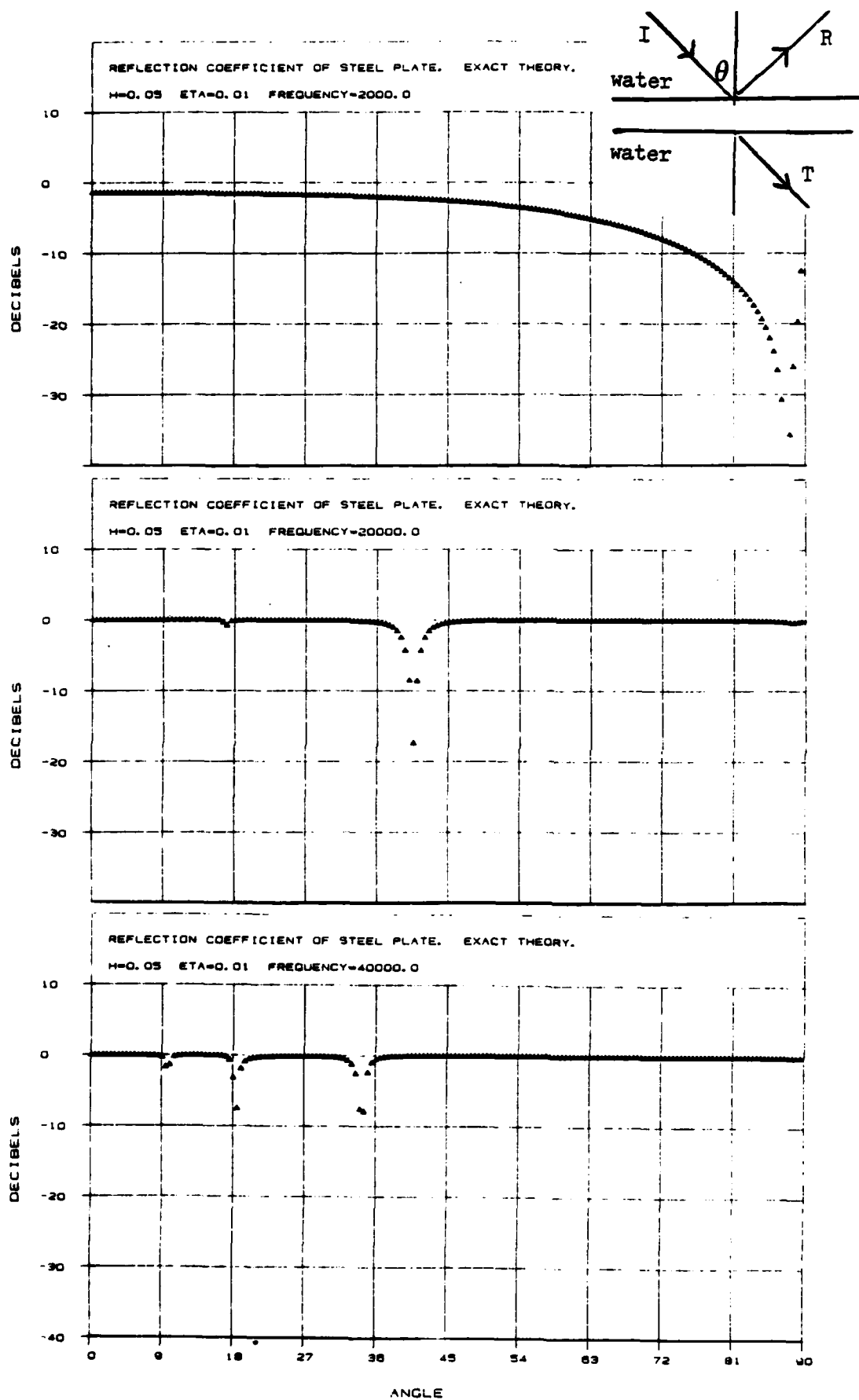
FIG.12  REFLECTION COEFFICIENT OF STEEL PLATE IN WATER
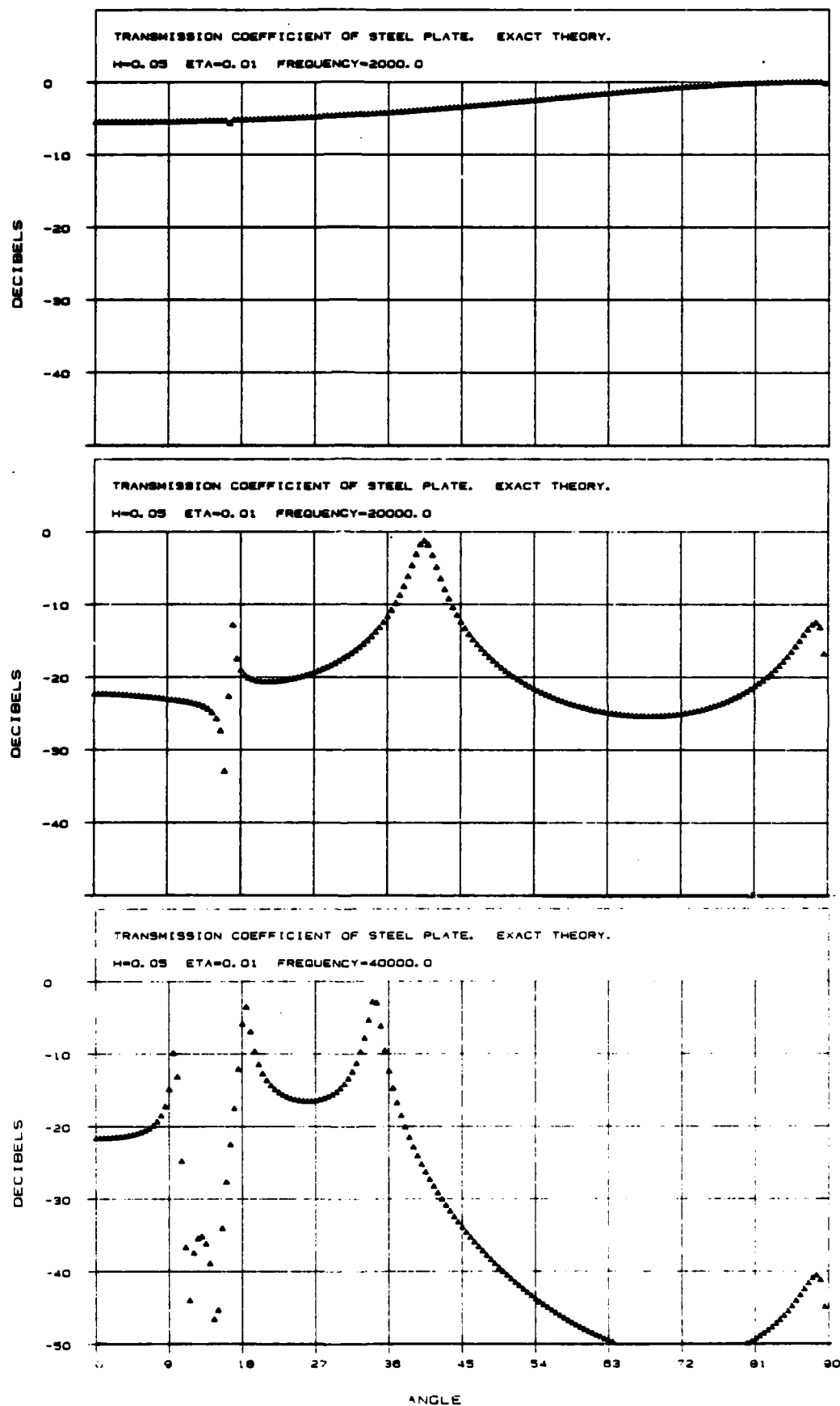
FIG.13  TRANSMISSION COEFFICIENT OF STEEL PLATE IN WATER

VERTICAL POINT FORCE EXCITATION
DYNAMIC RANGE = 40dB.   MAX = 206dB.

θ=90

Z
Y      X

θ=0
1kHz

water
θ
vacuum

p

50kHz

LONGITUDINAL POINT FORCE EXCITATION
DYNAMIC RANGE = 40dB.   MAX = 206dB.

θ=90

Z
Y      X

θ=0
1kHz

50kHz
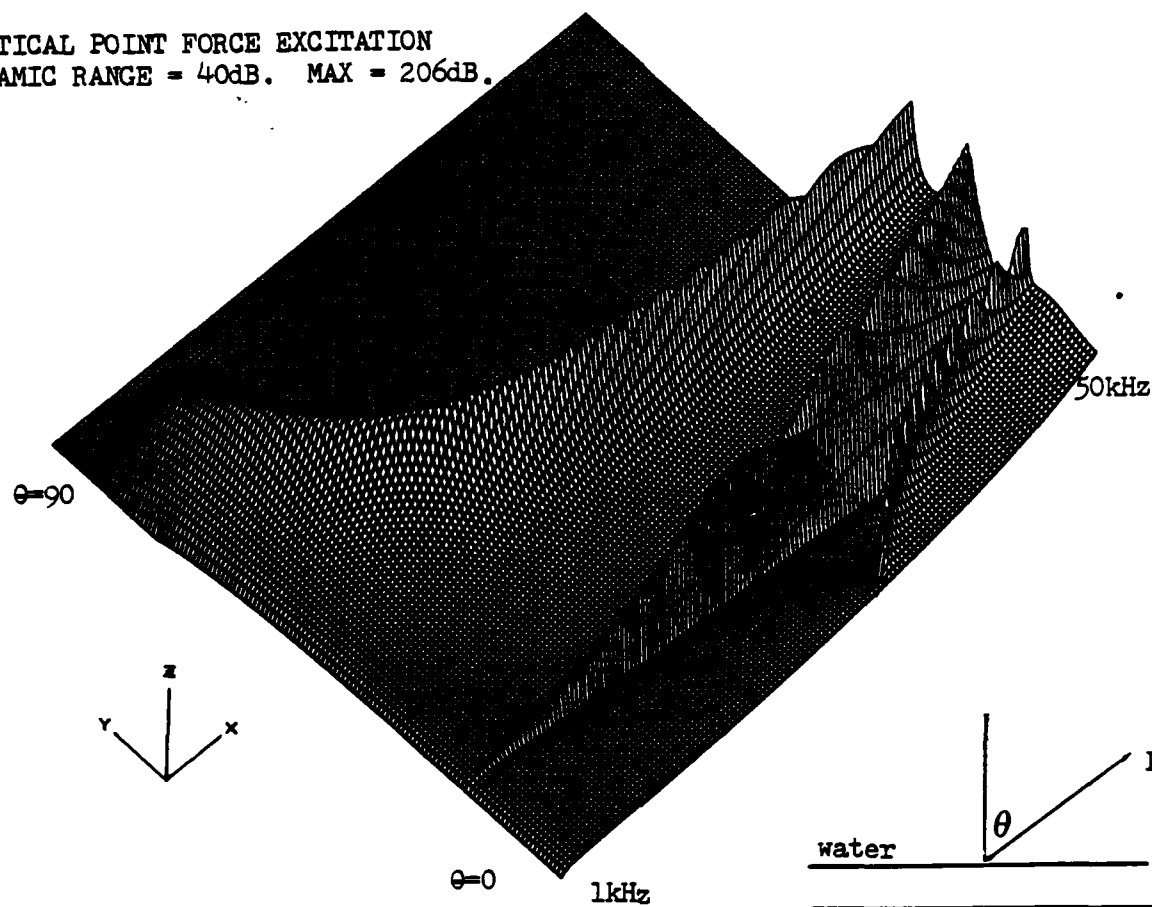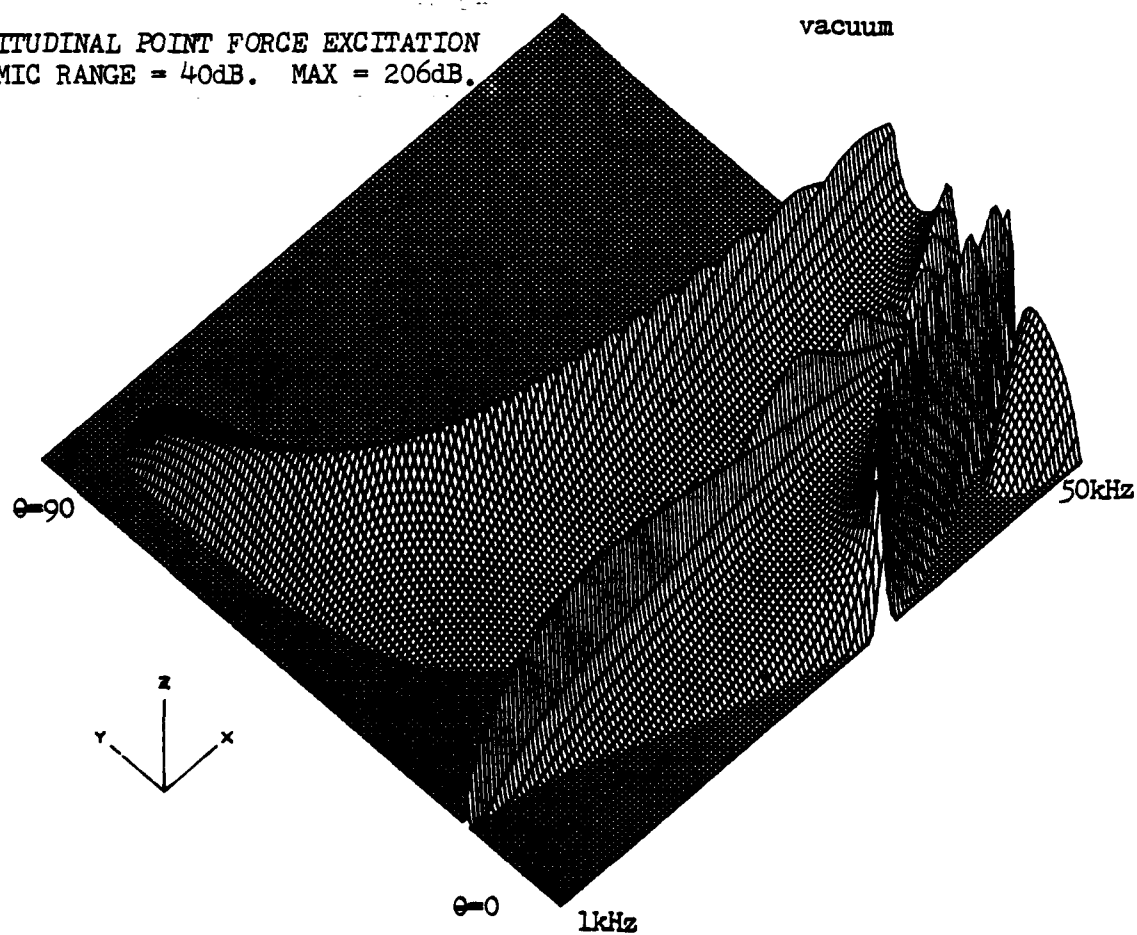
FIG.14   PERSPECTIVE PLOTS OF SOUND RADIATION
EXCITATION IS ON LOWER SURFACE

VERTICAL EXCITATION. CONTOURS IN MULTIPLES OF 10.
MAXIMUM LEVEL = 205.6 dB. MINIMUM LEVEL = 113.4 dB.
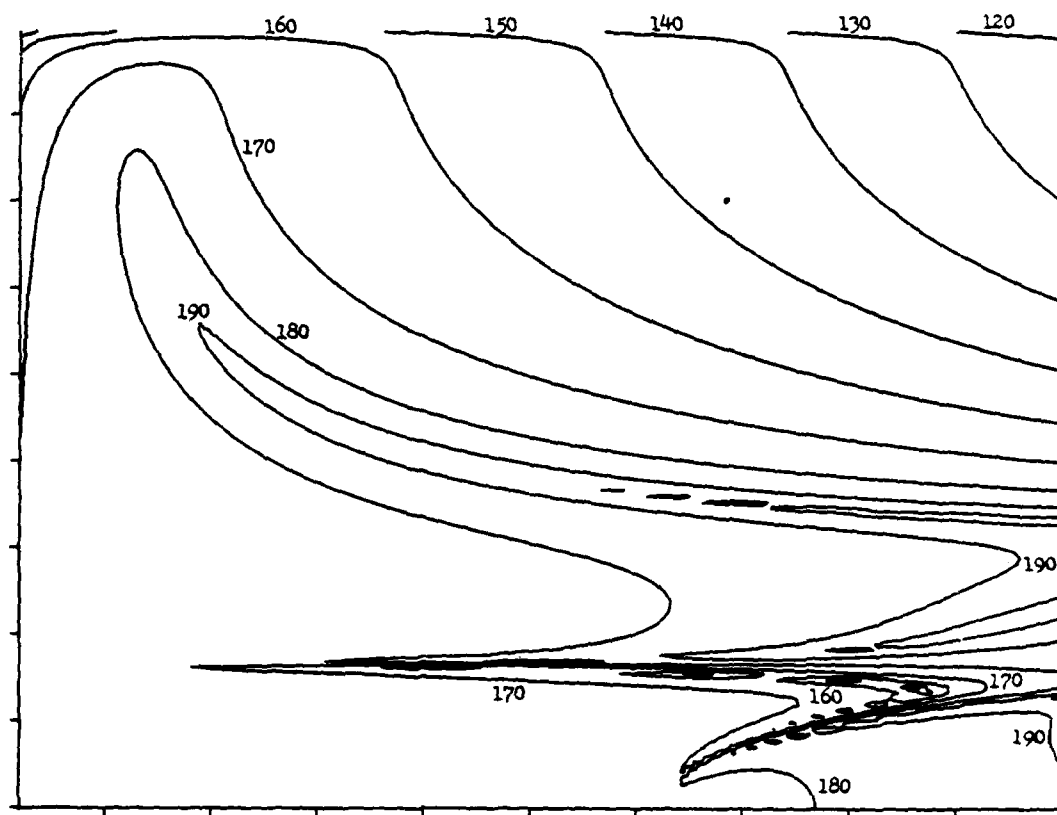
LONGITUDINAL EXCITATION. COUNTOURS IN MULTIPLES OF 10.
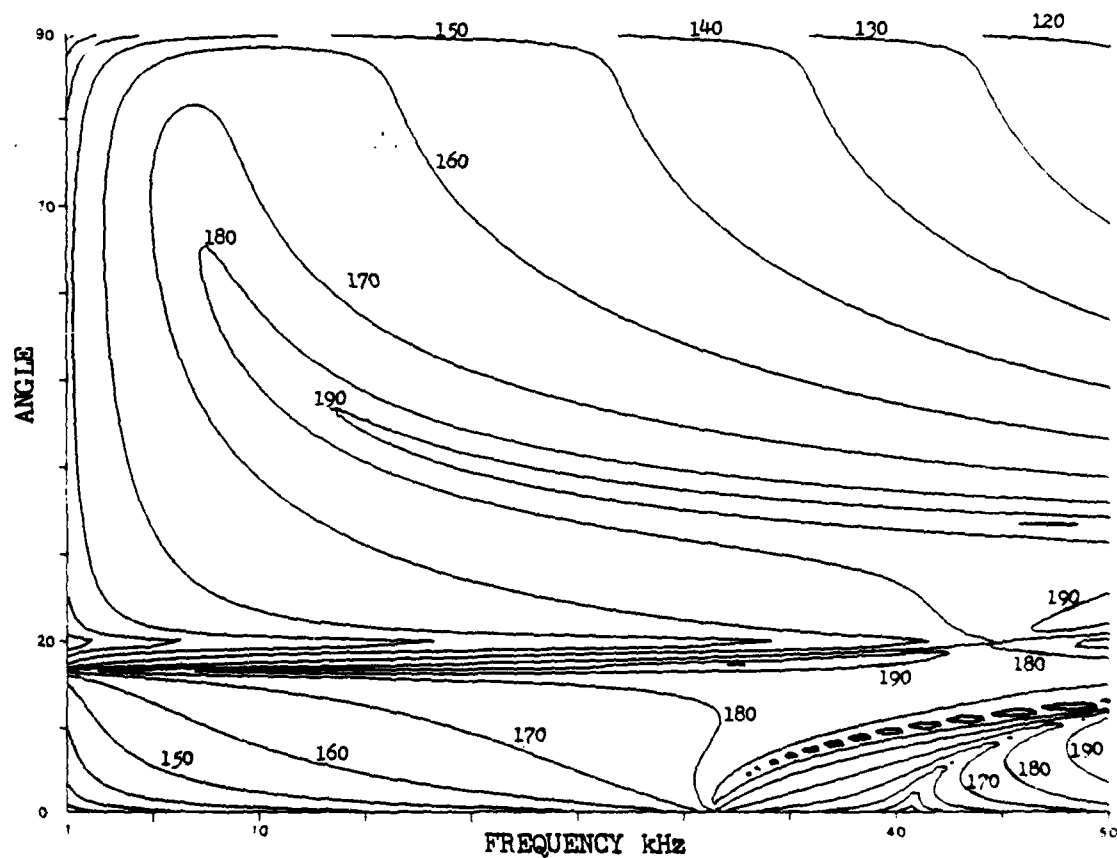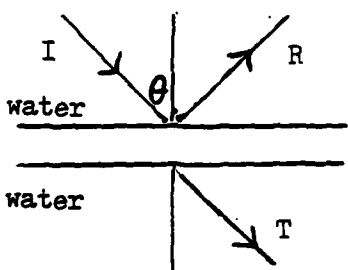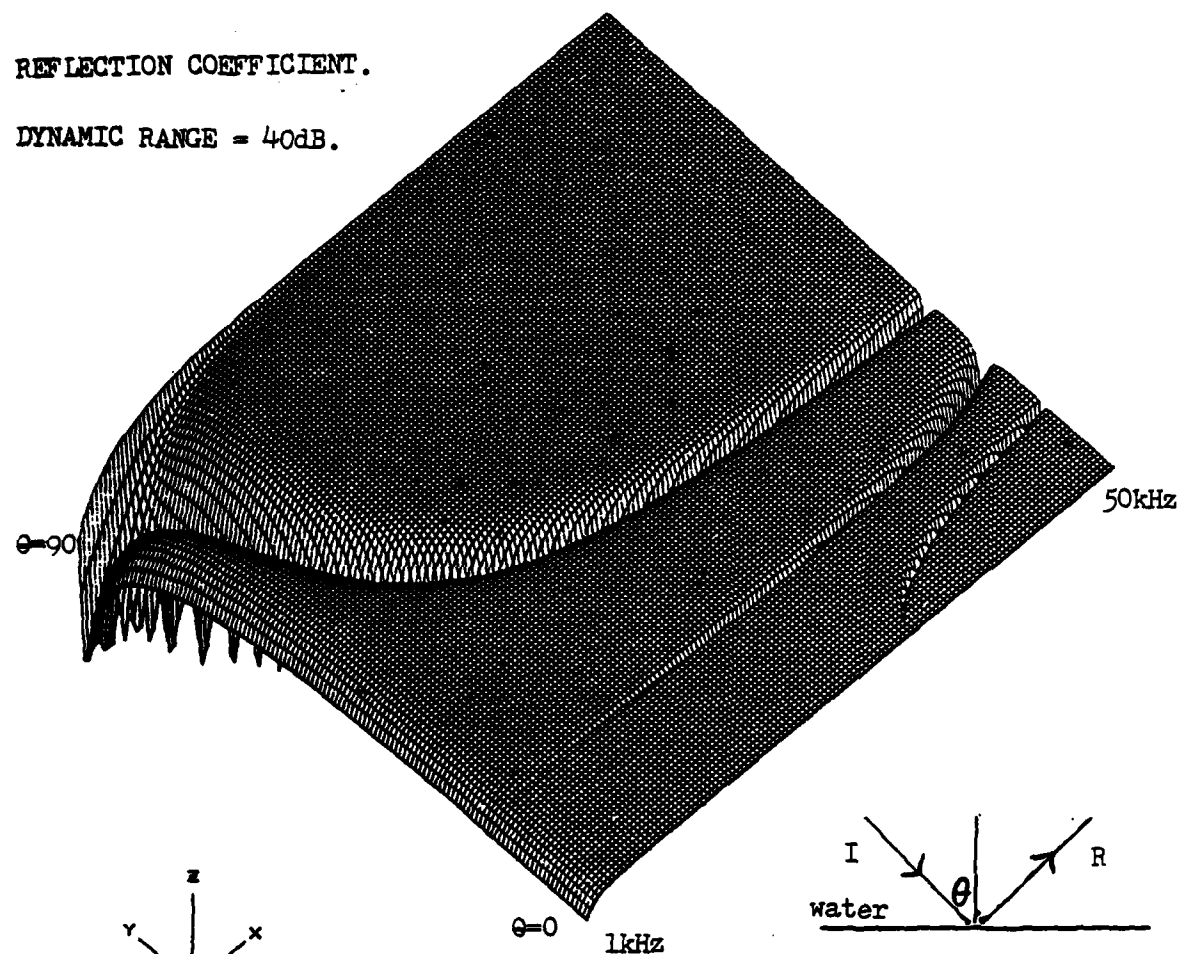MAXIMUM LEVEL = 205.7 dB. MINIMUM LEVEL = 112.2 dB.

FIG.15   CONTOUR PLOTS OF SOUND RADIATION
EXCITATION IS ON LOWER SURFACE

-27-

REFLECTION COEFFICIENT.

DYNAMIC RANGE = 40dB.



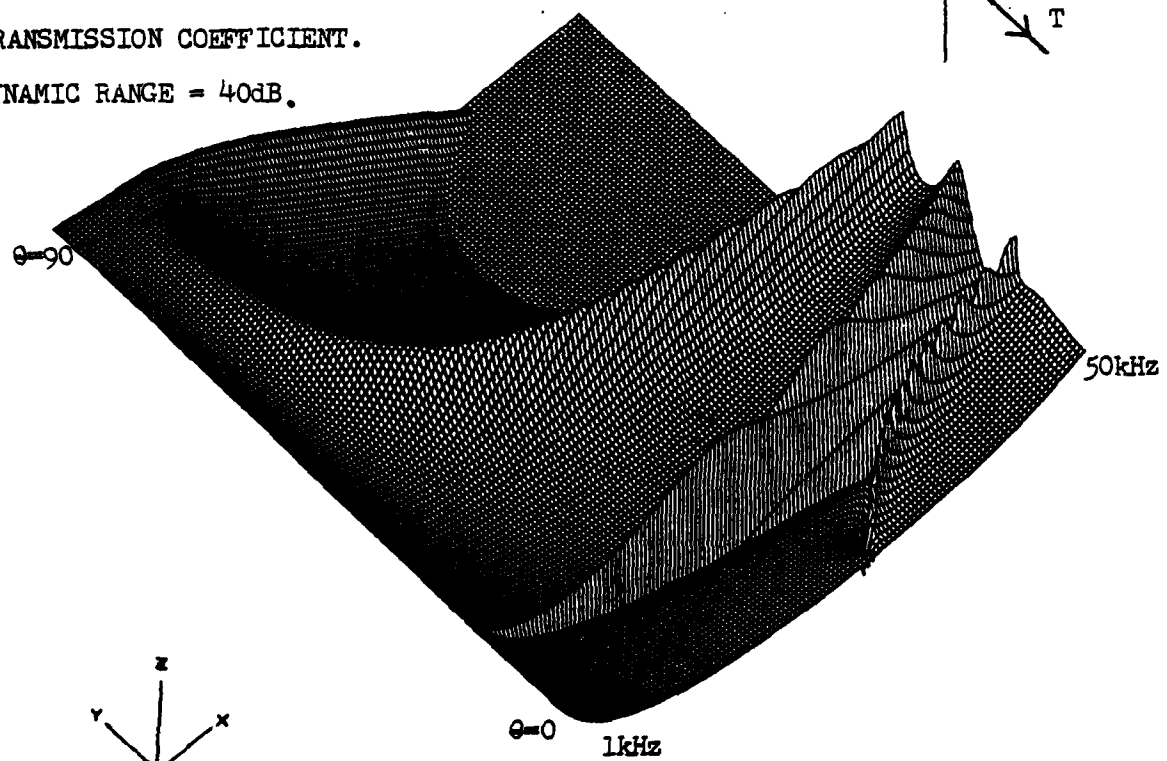TRANSMISSION COEFFICIENT.

DYNAMIC RANGE = 40dB.
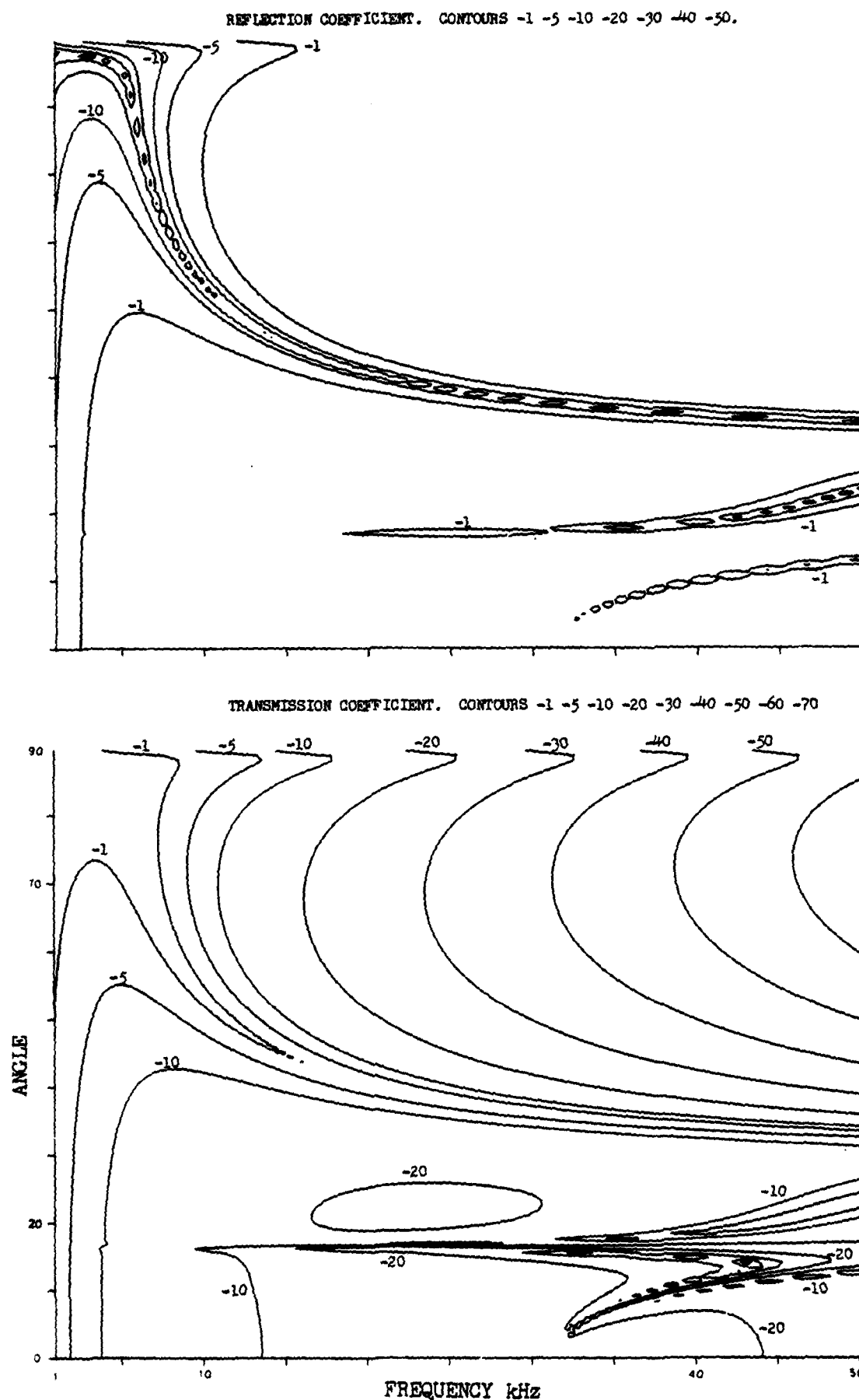


FIG.16   PERSPECTIVE PLOTS OF TRANSMISSION & REFLECTION

-28-

REFLECTION COEFFICIENT. CONTOURS -1 -5 -10 -20 -30 -40 -50.

TRANSMISSION COEFFICIENT. CONTOURS -1 -5 -10 -20 -30 -40 -50 -60 -70

FIG.17  CONTOUR PLOTS OF TRANSMISSION AND REFLECTION

-29-

END

FILMED

6-84

DTIC